Available online at www.sciencedirect.com
SCIENCE DIRECT®
Physics Letters A 344 (2005) 401–410
PHYSICS LETTERS A
www.elsevier.com/locate/pla

Signal detection for frequency-shift keying via short-time stochastic resonance

Fabing Duan [a], Derek Abbott [b,*]

[a] *Institute of Complexity Science, Department of Automation Engineering, Qingdao University, Qingdao 266071, PR China*
[b] *Centre for Biomedical Engineering (CBME) and School of Electrical & Electronic Engineering, University of Adelaide, Adelaide, SA 5005, Australia*

Received 3 March 2005; received in revised form 13 June 2005; accepted 22 June 2005

Available online 11 July 2005

Communicated by C.R. Doering

Abstract

A series of short-time stochastic resonance (SR) phenomena, realized in a bistable receiver, can be utilized to detect a train of information represented by signals that adopt frequency-shift keying (FSK). It is demonstrated that the values of noise intensity at resonance regions are close for adjacent periodic signals with an appropriate frequency separation. This establishes the possibility of decoding subthreshold or slightly suprathreshold M-ary FSK signals in bistable receivers. Furthermore, the mechanism of FSK signal detection via short-time SR effects is elucidated in terms of the receiver response speed. This phenomenon provides a possible mechanism for information processing in a bistable device operating in nonstationary noisy environments, where even the inputs appear over a short timescale or have a frequency shift.

Keywords: Bistable receiver; Short-time stochastic resonance; Frequency-shift keying; Receiver response speed

1. Introduction

Stochastic resonance (SR) is now a well established phenomenon wherein the response of a nonlinear system to a subthreshold periodic input signal can be enhanced by the assistance of noise [1–7]. Since a single-frequency sinusoidal input conveys little information content, this effect has been extended to aperiodic (i.e., broadband) input signals, leading to the term: aperiodic stochastic resonance (ASR) [8–16]. From the point of view of information transmission, an aperiodic information-bearing signal might be associated with analog (amplitude and frequency) modulated signals [17–21], or digitally modulated signals [10,12,20–22,24–29] within the context of SR effects. Digital pulse amplitude modulated signals have been intensively investigated for revealing new ASR phe-

* Corresponding author.
E-mail address: dabbott@eleceng.adelaide.edu.au (D. Abbott).

0375-9601/$ – see front matter
doi:10.1016/j.physleta.2005.06.113

nomena, suggesting novel applications [10,12,22,24–29]. Recently, a new type of electronic receiver based on SR properties has been proposed for retrieval of subthreshold digitally modulated signals that utilize frequency-shift keying (FSK) [20,21].

In the present Letter, the input information sequences are also represented by equal-energy orthogonal signal waveforms that differ in frequency, i.e., the FSK signals [20,21,37]. But, the prototype SR model, i.e., an overdamped bistable system [1–6,9–12,18,22,24–32], is adopted as a nonlinear receiver that decodes the received signals. In each symbol interval, FSK signals represent the digital information with a single-frequency periodic waveform, and the conventional SR-type phenomenon will appear in the presence of an appropriate amount of noise. Usually, conventional SR is characterized with a statistical measurement, e.g., signal-to-noise ratio, resulting from long-term observational data [1–16]. In contrast, we are more interested in the noise-enhanced effects that occur in each short-term duration of each symbol interval as the noise intensity increases—what we call the *short-time SR* phenomenon in this Letter. Due to the transient nature of the input waveform in each symbol interval, we decode the digital information with a rule based on zero crossing times, rather than a statistical measurement. We note that the input is an aperiodic signal and the noise-induced synchronization in a bistable receiver can be related to ASR effects in view of the long-term timescale of entire transmission time (over 5000 transmitted codes). Thus, an information measure, the percentage of bytes correctly decoded, is employed to quantify the performance of the bistable receiver. Here, short-time SR is emphasized as being in a short-term timescale of the symbol interval, whereas we are in a standard situation of ASR in the case of a long-term data statistics. Since the ASR phenomenon cannot cover all features of the detection of FSK modulated digital signals, short-time SR is claimed here in regard to the adaptive ability of a bistable receiver to the timescale and the frequency variations. Additionally, the short-time SR effect is consistent with detecting weak signals from a short data record [27], storing information in a short-term memory device [28] and exploring transient stimulus-locked coordinated dynamics in terms of mechanisms of short-term adaptation in sensory processing [36].

From a series of short-time SR effects, the input information contents can be deciphered at the output of the bistable receiver in terms of different signal frequencies. The SR effects realized in a nonlinear bistable receiver, as will be shown, are not sensitive to adjacent periodic signals with an appropriate frequency separation. In other words, the values of the noise intensity at resonance regions are close for two adjacent periodic signals. This nonlinear characteristic of a bistable receiver is then studied in detail for detecting M-ary FSK digitally modulated signals. It is also interesting to notice that, in addition to subthreshold FSK signal detection, this strategy can be extended to enhance the detection of slightly suprathreshold FSK signals. Furthermore, the response speed of bistable receivers, independent of the frequency of input signals, is theoretically deduced in Section 3. In view of the receiver response speed, the mechanism of M-ary FSK signal detection is explained. Finally, we suggest that short-time SR is not a trivial effect in signal detection, for example, in the detection of bipolar pulse signals with an unknown arrival time [29]. The short-time SR effect may also be of interest for bistable electronic or optical devices operating in nonstationary noisy environments, regardless of the short timescale or the frequency shift.

2. Bistable receiver and M-ary FSK signal detection

An input information-bearing sequence $\{I\}$ is mapped onto the M-ary FSK signal $S(t)$ as

$$S(t) = A\cos(2\pi f_m t), \quad m = 1, 2, \ldots, M, \tag{1}$$

for $(n-1)T \leqslant t \leqslant nT$, $n = 1, 2, \ldots$. Here, A is the amplitude, $\{f_m, m = 1, 2, \ldots, M\}$ denotes the set of M possible carrier frequencies corresponding to $M = 2^k$ possible k-bit symbols, and T is the symbol interval. The received signal $R(t)$ is

$$R(t) = A\cos(2\pi f_m t + \phi_m) + \eta(t), \tag{2}$$

where ϕ_m are phase shifts of carrier frequencies f_m induced by the channel, and the background noise $\eta(t)$ is additive Gaussian white noise with autocorrelation $\langle \eta(t)\eta(0)\rangle = 2D\delta(t)$ and zero-mean. Here, D denotes the noise intensity. Next, $R(t)$, as shown in Fig. 1, is

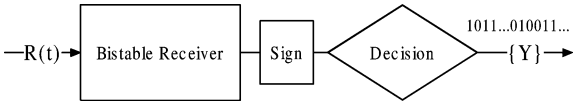

Fig. 1. Bistable receiver and demodulator for M-ary FSK signals.

applied to a bistable dynamic receiver characterized as

$$\tau_a \frac{dx(t)}{dt} = x(t) - \frac{x^3(t)}{X_b^2} + R(t), \tag{3}$$

with receiver parameters $\tau_a > 0$ and $X_b > 0$ [22]. Here, τ_a is related to the system relaxation time. The dynamics of Eq. (3) is derived from the symmetrical double-well potential $V_0(x) = -x^2/2 + x^4/(4X_b^2)$, having the two minima $V_0(\pm X_b) = -X_b^2/4$. Parameters τ_a and X_b have the units of time and signal amplitude respectively, and define natural scales associated with the process of Eq. (3) [24]. The term "subthreshold" associated with the input signal amplitude requires that $A < 2X_b/\sqrt{27}$, so that the input $S(t)$ alone is too weak to induce transitions at the output of bistable receiver. Otherwise, an input signal is "suprathreshold" for bistable receivers [5,22,24].

We are interested in recovering the successive input information bits, from the observation of the system state $x(t)$. Moreover, our focus is on the signal frequency rather than the waveforms at the output of the bistable receiver, due to the information content being represented by different frequencies. In this Letter, we numerically integrate the stochastic differential equation of Eq. (3) using a Euler–Maruyama discretization method with a small sampling time step $\Delta t \ll \tau_a$ [38]. The demodulation method, as shown in Fig. 1, is implemented with zero crossing times N_m. If the bistable receiver follows the periodic signal correctly by the assistance of noise, the zero crossing times N_m of modulated signal $S(t)$ should be $2f_mT$ in each symbol interval T. At the output of the bistable receiver, however, the zero crossing times N_m will be in the vicinity of $2f_mT$ even in the resonance region of noise, as shown in Fig. 2(c). For simplicity, the bytes represented by the corresponding input signals with frequency f_m are decoded as

$$\begin{aligned} &(f_{m-1} + f_m)T \leqslant N_m < (f_m + f_{m+1})T, \quad \text{or} \\ &(2f_m - \Delta f)T \leqslant N_m < (2f_m + \Delta f)T, \end{aligned} \tag{4}$$

with the frequency separation $\Delta f = f_{m+1} - f_m$ for $m = 1, 2, \ldots, M$ and $\Delta f = 1/(2T)$ represents the

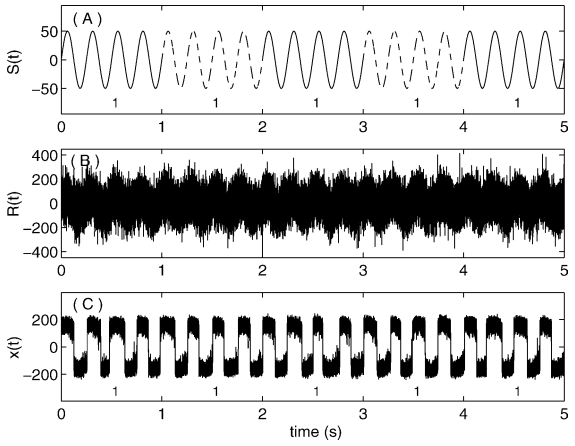

Fig. 2. Time evolution of binary FSK signal transmission in a bistable receiver. (a) $S(t) = 50\cos(8\pi t)$ representing binary digit 1 (or 0). Here, $S(t)$ is plotted with solid and dashed curves alternately in each symbol interval of $T = 1$ s, and should be considered as segmented signals rather than a continuous wave in the whole transmission time. (b) The received signal is $R(t)$. Here, the phase shift ϕ_m induced by the channel is $\pi/6$ and the noise intensity $D = 0.8$ V^2/Hz. (c) The bistable receiver output signal $x(t)$ with parameters $\tau_a = 1/3000$ s and $X_b = 150$ V. The decoded binary bits are depicted in terms of the zero crossing times. The sampling time $\Delta t = 10^{-5}$ s.

minimum frequency separation between adjacent signals for orthogonality of the M-ary FSK signals. Then, the output information sequence Y is decoded. Now, this system of Eq. (3) with a digital input and output, can be viewed as an information channel transmitting digital data. By comparing sequences I and Y, the measure of the percentage P of bytes correctly decoded will be employed to quantify the performance of this nonlinear information channel. We shall show that this transmission of information can be assisted by additive noise in each symbol interval, a property we interpret as a short-time SR effect.

As the noise intensity D increases from zero to the resonance point or the resonant region, shown in Fig. 2(c), the switching between wells is made to agree closely with the input periodic signal, resulting from the combined action of noise and periodic signal in a bistable receiver. This synchronization phenomenon in each symbol interval of T is called the short-time SR effect. In Fig. 2(a), the input periodic signals in each short data record of time length T have the same frequency, which can represent a particular input binary sequence $I = [1\ 1\ \ldots\ 1]$ or $I = [0\ 0\ \ldots\ 0]$. The res-

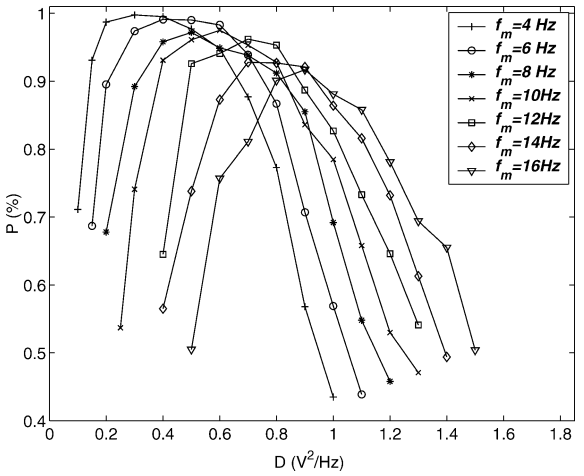

Fig. 3. The percentage P of correctly decoded bytes as a function of noise intensity D. In each symbol interval of length T, the input signal $S(t) = 50\cos(2\pi f_m t)$ has a frequency f_m (as marked in the legend). The statistical values of P are computed numerically from 5000 transmitted codes. Here, receiver parameters $\tau_a = 1/3000$ s and $X_b = 150$ V. Also, $T = 1$ s and $\Delta t = 10^{-5}$ s.

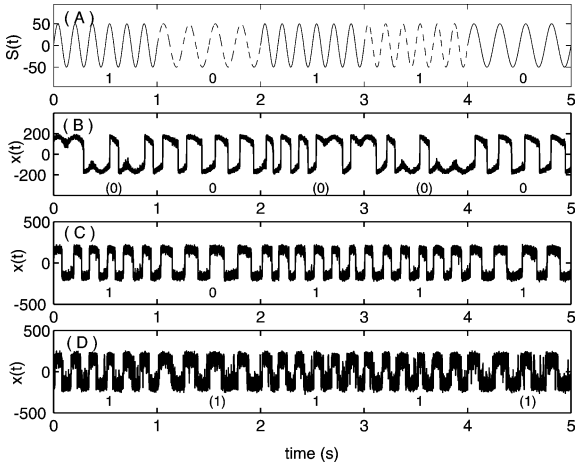

Fig. 4. (a) A binary FSK signal $S(t) = 50\cos(2\pi f_m t)$ with carrier frequencies 4 Hz and 6 Hz representing binary code words 0 and 1, respectively. Parameters are $\tau_a = 1/3000$ s and $X_b = 150$ V. Here, (b), (c) and (d) are plots of receiver outputs $x(t)$ at $D = 0.1$ V^2/Hz, $D = 0.37$ V^2/Hz and $D = 1.1$ V^2/Hz. The erroneous decoded bytes are bracketed. The phase shift ϕ_m induced by the channel is $\pi/6$. Also, $T = 1$ s and $\Delta t = 10^{-5}$ s.

onance curves, illustrated in Fig. 3, are distinct from the previous conventional SR form: the SR effect is manifested and observed in each symbol interval T, rather than the entire transmission time. Numerical results of Fig. 3 show that the percentage P of correct switching events, as the noise intensity D increases, presents a typical SR characteristic. Especially worthy of note is that the resonant regions or points of two adjacent frequencies are close. This indicates that the bistable receiver is not sensitive to the frequency change of periodic input signals. Thus, it is possible to use a bistable receiver to decode M-ary information represented by periodic signals with different frequencies, i.e., FSK digitally modulated signals. This possibility is immediately demonstrated in Figs. 4 and 6 with numerical examples of binary and 4-ary FSK signal detection, respectively. In different symbol intervals of length T, the bistable receiver can follow the input periodic signals with adjacent frequencies in an appropriate noise intensity region. The percentage P, as shown in Figs. 5 and 7, is a nonmonotonic function of noise intensity D for different binary and 4-ary FSK signals, resulting from a series of short-time SR effects.

We also note that the above detection strategy can be extended to detect slightly suprathreshold FSK signals for bistable receivers. The signal $S(t) = 58\cos(2\pi f_m t)$, as illustrated in Fig. 8(a), are with carrier frequencies 4, 6, 8 and 10 Hz. Here, the amplitude $A = 58 > 2X_b/\sqrt{27}$ is slightly suprathreshold for the bistable receiver with $X_b = 150$ V, since the deterministic switching can occur in the presence of the signal alone. However, this suprathreshold input $S(t)$ is fast for the receiver with the parameter $X_b = 150$ V, and the dynamical bistable receiver output cannot cross the zero threshold in one period of $1/f_m$ without the help of noise, as shown in Fig. 8(b). In such a condition, the noise plays a constructive role, by spurring the output switching of the system, helping to better follow the transitions present in the fast suprathreshold input [23,24], as seen in Fig. 8(d). This temporal effect is a residual SR phenomenon occurring in one symbol interval of T, wherein a slow dynamical system exploits noise to track the variations imposed by a fast slightly suprathreshold input [23,24]. In the view of the short timescale of effects, we also associate it with the short-time SR in this Letter. The corresponding percentage P, as shown in Fig. 9, manifests a representative SR-type behavior as noise intensity D varies for different 4-ary suprathreshold FSK signals. For $M > 4$, a parallel bank of receivers can be designed

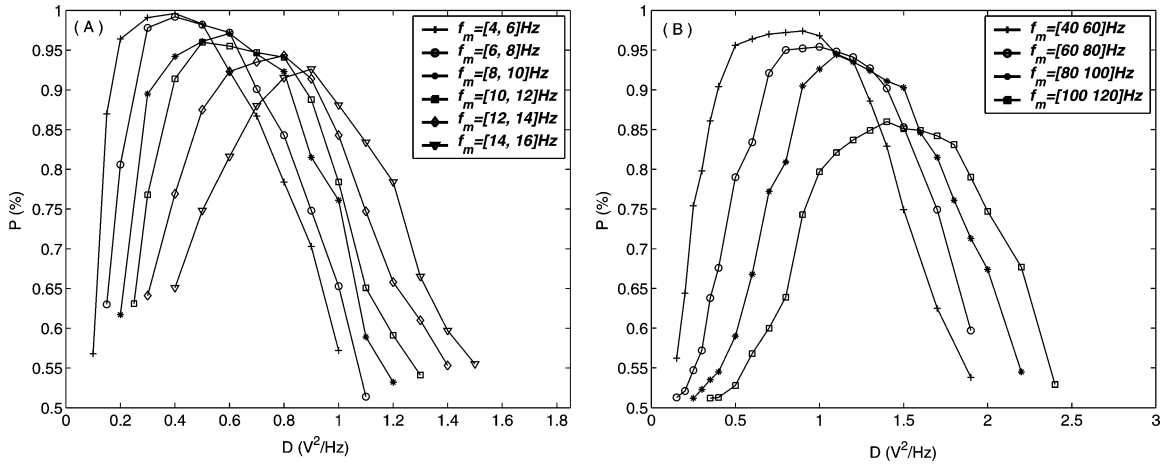

Fig. 5. Plots of the percentage P as a function of D for binary FSK signal detection in bistable receivers. The statistical values of P are obtained from 5000 transmitted codes. The corresponding carrier frequencies are given in plots. (a) The receiver parameters are $\tau_a = 1/3000$ s and $X_b = 150$ V. Here, $T = 1$ s and $S(t) = 50\cos(2\pi f_m t)$. (b) The receiver parameters are $\tau_a = 1/10000$ s and $X_b = 380$ V. Here, $T = 0.1$ s and $S(t) = 140\cos(2\pi f_m t)$. The sampling time is $\Delta t = 10^{-5}$ s.

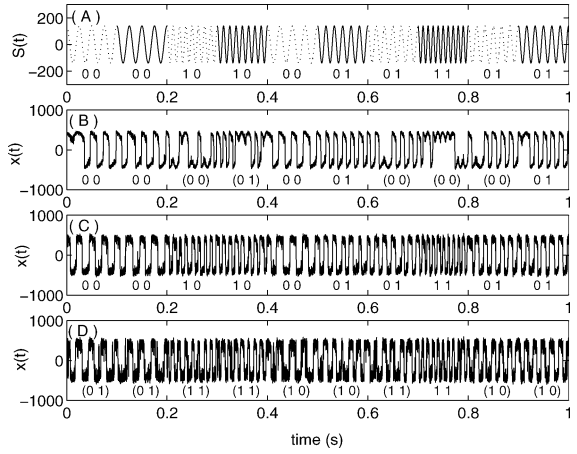

Fig. 6. (a) A 4-ary FSK signal $S(t) = 140\cos(2\pi f_m t)$ with carrier frequencies 40, 60, 80 and 100 Hz, representing 4-ary code words 00, 01, 10 and 11, respectively. The receiver parameters are $\tau_a = 10^{-4}$ s and $X_b = 380$ V. Here, (b), (c) and (d) are plots of receiver outputs $x(t)$ at $D = 0.25$ V^2/Hz, $D = 1.0$ V^2/Hz and $D = 2.4$ V^2/Hz. The erroneous decoded bytes are bracketed. The phase shift ϕ_m induced by the channel is $\pi/6$. Here, $T = 0.1$ s and $\Delta t = 10^{-5}$ s.

for this complicated task, with different receiver parameters and improved deciphering scheme.

Next, we investigate the behavior of the bistable receiver when the phase shift is not known or random. In Fig. 10, the percentage P of correctly decoded bytes are illustrated as the phase shift ϕ takes values of zero, $\pi/6$, $\pi/4$, $\pi/2$ and $3\pi/4$. We observe that the percentage P is almost same for different phase shifts in detecting 4-ary FSK signals. This indicates that the bistable receiver is robust to the phase shift and applicable when the carrier phase is unknown at the receiver and no attempt is made to estimate its values. In the presence of periodic inputs, the receiver dynamics is derived from the antisymmetric double-well potential $V(x,t) = V_0(x) - Ax\cos(2\pi f_m t + \phi_m)$. The zero crossing times N_m, i.e., barrier crossings, are counted as the noise-induced transitions between the right and the left well, while the wells are raised and lowered successively. In terms of the rule of Eq. (4), unknown or random phase shift seems not to affect this detection strategy, because the zero crossing times are decided as $(f_{m-1} + f_m)T \leqslant N_m < (f_m + f_{m+1})T$, rather than $N_m = 2f_m T$, standing for the correctly decoded bytes represented by the input signals frequency f_m. Note that the zero crossing times N_m are obtained by over-sampling the receiver output $x(t)$. This interesting problem deserves further study in the future.

3. The mechanism of FSK signal detection in a bistable receiver

In this section we shall now attempt to explore the physical mechanism of FSK signal detection in a

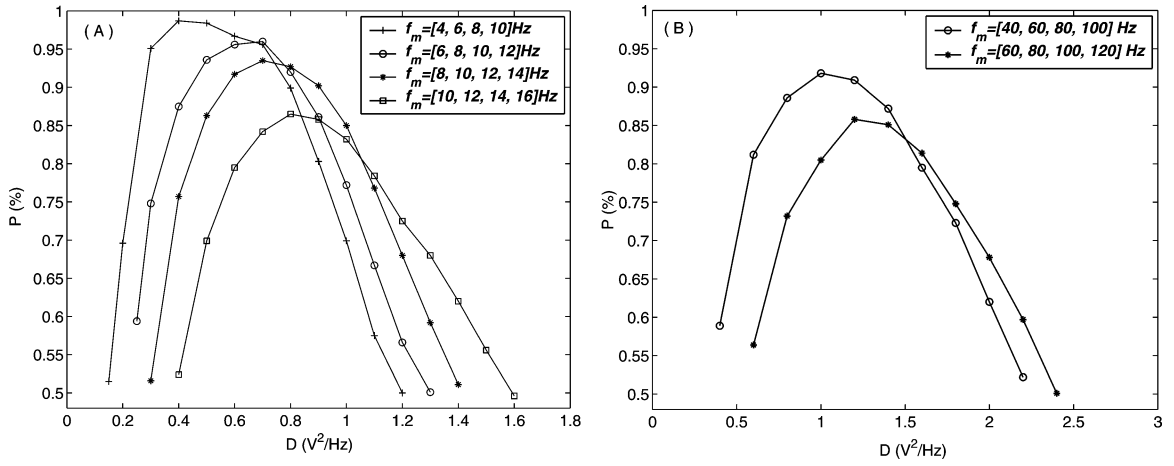

Fig. 7. Plots of the percentage P as a function of D for the 4-ary FSK signal transmission in bistable receivers. The corresponding carrier frequencies are given in the legend of the above plots. Graphs (a) and (b) are with the same parameters as in Fig. 5, respectively.

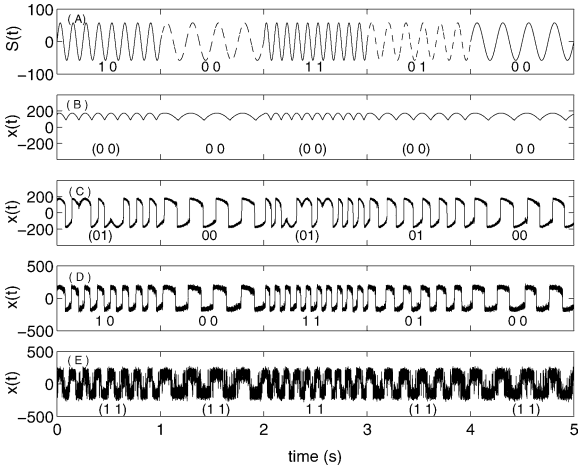

Fig. 8. (a) A 4-ary slightly suprathreshold FSK signal $S(t) = 58\cos(2\pi f_m t)$ with carrier frequencies 4, 6, 8 and 10 Hz, representing 4-ary code words 00, 01, 10 and 11, respectively. The receiver outputs $x(t)$ at (b) $D = 0$ V^2/Hz, erroneous decoded bytes are bracketed; (c) $D = 0.025$ V^2/Hz; (d) $D = 0.31$ V^2/Hz, optimum noise intensity; (e) $D = 1.5$ V^2/Hz, too much noise. The phase shift ϕ_m induced by the channel is $\pi/7$. Here, $\Delta t = 10^{-5}$ s, $\tau_a = 1/3000$ s and $X_b = 150$ V.

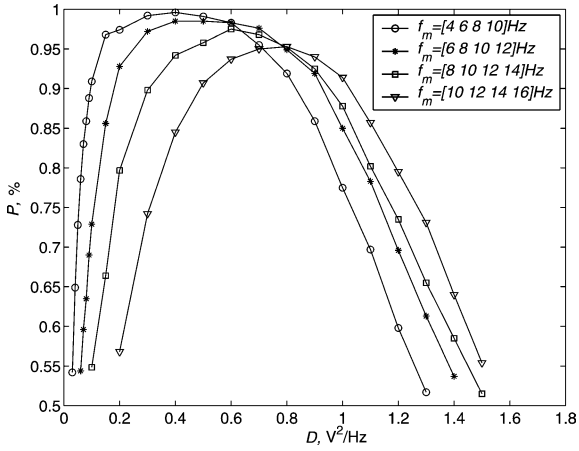

Fig. 9. The percentage P of correctly decoded bytes as a function of noise intensity D for the 4-ary slightly suprathreshold FSK signal detection in bistable receiver. The corresponding parameters are as same as in Fig. 8.

bistable receiver, by exploiting an approximation of the nonstationary probability density of Eq. (3) and its temporal relaxation. The temporal relaxation of the nonstationary probability density, termed the receiver response speed λ_1, will be demonstrated as being independent of the input signal frequency. The study of system response speed allows us to explicitly have a deeper understanding of the FSK signal detection in a nonlinear bistable receiver.

In numerical simulations, we numerically sample a sinusoidal signal with zero-hold and sampling time $\Delta t \ll \tau_a$ [10,22,24,25,29]. Hence, in a sampling interval of Δt, the system of Eq. (3) is subjected to a constant amplitude $s(t) = A_i$ $(i\Delta t \leqslant t < (i+1)\Delta t$, $i = 0, 1, 2, \ldots)$, as shown in Fig. 11. In the presence of noise $\eta(t)$, the statistically equivalent description for the corresponding probability density $\rho(x,t)$ is gov-

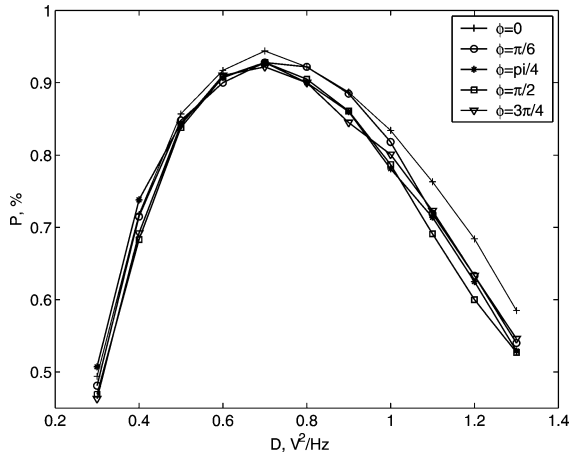

Fig. 10. Plot of the percentage P as a function of D for the 4-ary FSK signal transmission in bistable receivers with different phase shifts $\phi = 0$, $\pi/6$, $\pi/4$, $\pi/2$ and $3\pi/4$. The input signal $S(t) = 50\cos(2\pi f_m t)$ has carrier frequencies 4, 6, 8 and 10 Hz. The receiver parameters are $\tau_a = 1/3000$ s and $X_b = 150$ V. Here, $T = 1$ s and $\Delta t = 10^{-5}$ s.

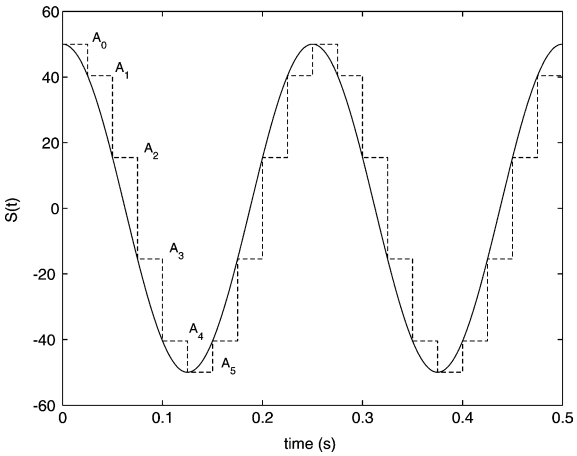

Fig. 11. A sinusoidal signal with zero-hold sampling.

erned by the Fokker–Planck equation

$$\tau_a \frac{\partial \rho(x,t)}{\partial t} = \left[\frac{\partial}{\partial x}V'(x) + \frac{D}{\tau_a}\frac{\partial^2}{\partial x^2}\right]\rho(x,t), \tag{5}$$

where $V'(x) = -(x - x^3/X_b^2 + A_i)$ and the Fokker–Planck operator $L_{\mathrm{FP}} = \frac{\partial}{\partial x}V'(x) + \frac{D}{\tau_a}\frac{\partial^2}{\partial x^2}$. $\rho(x,t)$ obeys the natural boundary conditions such that it vanishes at large x for any t [39]. The steady-state solution of Eq. (5), for a constant input at A_i, is given by

$$\rho(x) = \lim_{t\to\infty}\rho(x,t) = C\exp\bigl[-\tau_a V(x)/D\bigr], \tag{6}$$

where C is the normalization constant [39]. As the sampling amplitude A_i varies, we encounter the nonstationary solution $\rho(x,t)$ of the Fokker–Planck equation, i.e., Eq. (5). This analysis is performed in Appendix A. We show in Appendix A that the nonstationary solution $\rho(x,t)$ can be expanded as an asymptotic representation of eigenfunctions $u_i(x)$ and eigenvalues λ_i

$$\rho(x,t) = \sum_{i=0}^{n} C_i u_i(x) \times \exp\bigl[-\tau_a V(x)/(2D)\bigr]\exp[-\lambda_i t], \tag{7}$$

where C_i are normalization constants for $i = 0, 1, 2, \ldots$.

Specifically, the inverse of the minimal positive eigenvalue λ_1 is a measure of the slowest time taken by the bistable receiver to tend to the steady-state solution of Eq. (6). In other words, λ_1 is the speed of the bistable receiver tracing the variety of input signals, whence our term "receiver response speed." Fig. 12 shows the behavior of the receiver response speed in the related regions. Note that the receiver response speed λ_1, for a fixed bistable receiver with parameters τ_a and X_b, is a monotonically increasing function of signal amplitude $|A|$ and noise intensity D, but independent of the input signal frequency f_m, as indicated in Eq. (A.8). When the noise intensity D is too small, the receiver cannot follow the input signal correctly, as shown in Figs. 4(b) and 6(b). However, in the resonant regions of noise intensity D, λ_1 is large enough to make the receiver output $x(t)$ reach the steady-state, whereas the signal amplitude continually changes from $\pm A$ to $\mp A$ at different but adjacent carrier frequencies f_m. This indicates detecting weak FSK modulated signals is possible in a bistable receiver, as seen in Figs. 4(c) and 6(c). After the noise intensity D is beyond the resonance region, λ_1 is too fast to catch up with the fluctuations induced by noise, resulting in the loss of synchronization, as shown in Figs. 4(d) and 6(d). Especially, we argue that the so-called suprathreshold FSK signal $S(t) = A\cos(2\pi f_m t)$ $(A > 2X_b/\sqrt{27})$ is mainly subthreshold and slightly suprathreshold as illustrated in Fig. 8, since the amplitude $|A|$ changes in each period. Therefore, the system response speed λ_1 is in such a

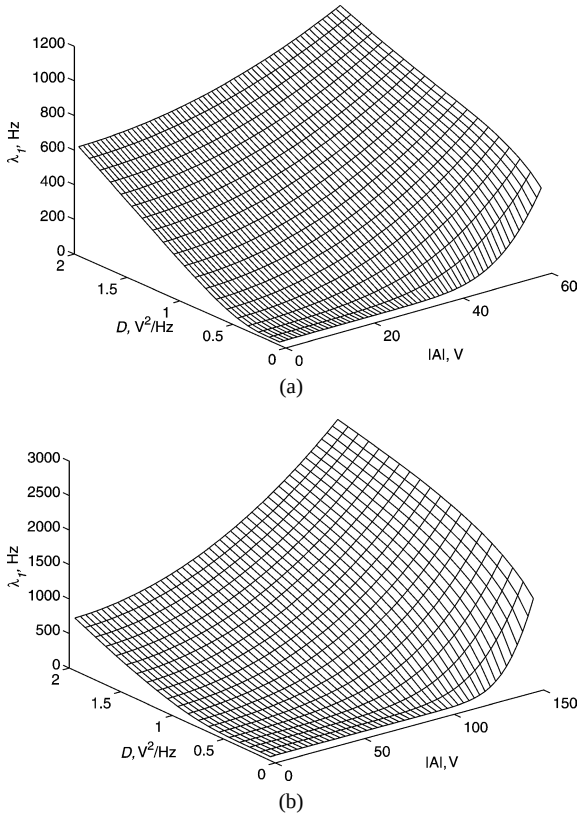

Fig. 12. The receiver response speed λ_1 as a function of signal amplitude $|A|$ and noise intensity D for the receiver with parameters (a) $\tau_a = 1/3000$ s and $X_b = 150$ V and (b) $\tau_a = 10^{-4}$ s and $X_b = 380$ V. The slightly suprathreshold region of $|A|$ is $|A| = 2X_b/\sqrt{27} + \varepsilon$ and ε is a small value.

region that the receiver can follow the variation of input more correctly, even if the input amplitude $|A|$ is slightly suprathreshold.

The receiver response speed λ_1 contributes to the mechanism of detecting weak FSK modulated signals in a bistable receiver: within a reasonable region of noise intensity, the receiver responds synchronously to the input periodic signal, regardless of the short-term timescale of symbol interval T or the frequency shift of signals (i.e., the different carrier frequencies f_m). Therefore, the SR effect realized in a symbol duration T, i.e., the short-time SR effect, can be utilized to convey or store the digital data [27,28]. Additionally, noise-enhanced frequency discrimination was reported in Ref. [33], and the frequency robust characteristic of the bistable model was also verified in Ref. [29] in detail.

4. Discussion and conclusion

A detection strategy for FSK digitally modulated signals with a nonlinear bistable receiver was analyzed. It was numerically demonstrated that the resonance values of noise intensity appear closely for FSK modulated signals with adjacent frequencies. Assuming a demodulation method of the zero crossing times, a series of SR effects appearing in each symbol interval—what we call short-time SR—provide the possibility of detecting subthreshold and slightly suprathreshold M-ary FSK signals in bistable receivers. In order to understand the mechanism of FSK signal detection more deeply, we introduce the receiver response speed, i.e., a theoretical measure for the receiver tending to a steady-state. In the resonant region, the receiver response speed is fast enough to capture a variety of input periodic signals, regardless of the frequency difference and the short-term timescale of each symbol interval.

Finally, we argue that the short-time SR effect might be a possible detection strategy in neurodynamics, as the stimulus exists in a short time duration or has frequency shift [27,28,33–35]. This is an open question and currently under study.

Acknowledgements

We gratefully thank the anonymous reviewers for their constructive comments and suggestions. Funding from the Australian Research Council (ARC) is gratefully acknowledged. This project is also sponsored by Natural Science Foundation of Shandong Province of PR China (Y2002G01).

Appendix A. Receiver response speed and nonstationary probability density model

In Eq. (5), the Fokker–Planck operator $L_{\mathrm{FP}} = \frac{\partial}{\partial x}V'(x) + \frac{D}{\tau_a}\frac{\partial^2}{\partial x^2}$ is not a Hermitian operator [39]. We rescale the variables as

$$\bar{X}_b = X_b/\sqrt{D/\tau_a}, \qquad \bar{A}_i = A_i/\sqrt{D/\tau_a},$$
$$\tau = t/\tau_a, \qquad y = x/\sqrt{D/\tau_a}, \tag{A.1}$$

Eq. (5) becomes

$$\frac{\partial \rho(y,\tau)}{\partial \tau} = \left[\frac{\partial}{\partial y}V'(y) + \frac{\partial^2}{\partial y^2}\right]\rho(y,\tau), \tag{A.2}$$

where $V'(y) = -(y - y^3/\bar{X}_b^2 + \bar{A}_i)$. The steady-state solution of Eq. (A.2) is given by

$$\rho(y) = \lim_{\tau\to\infty}\rho(y,\tau) = C\exp\bigl[-V(y)\bigr], \tag{A.3}$$

where C is the normalization constant. A separation ansatz for $\rho(y,\tau)$ [39],

$$\rho(y,\tau) = u(y)\exp\bigl[-V(y)/2\bigr]\exp(-\lambda\tau), \tag{A.4}$$

leads to

$$Lu = -\lambda u, \tag{A.5}$$

with a Hermitian operator $L = \frac{\partial^2}{\partial y^2} - [\frac{1}{4}V'^2(y) - \frac{1}{2}V''(y)]$. The functions $u(y)$ are eigenfunctions of the operator L with the eigenvalues λ. Multiplying both sides of Eq. (A.5) by $u(y)$ and integrating it, yields

$$\lambda = \frac{\int_{-\infty}^{+\infty}\{u'^2(y) + u^2(y)[\frac{1}{4}V'^2(y) - \frac{1}{2}V''(y)]\}\,dy}{\int_{-\infty}^{+\infty}u^2(y)\,dy}, \tag{A.6}$$

where eigenfunctions $u(y)$ satisfy the boundary conditions of $u(y)$ and $u'(y)$ tending to zero as $y \to \pm\infty$. The eigenvalue problem of Eq. (A.5) is then equivalent to the variational problem consisting of finding the extremal values of the right side of Eq. (A.6) [25,39]. The minimum of this expression is then the lowest eigenvalue $\lambda_0 = 0$, corresponding to the steady-state solution of Eq. (A.3) [39]. We adopt here eigenfunctions $u(y) = p(y)\exp[-V(y)/2]$ and $p(y) \neq 0$, Eq. (A.6) becomes

$$\lambda = \left\{\int_{-\infty}^{+\infty}\left\{p'^2(y) + \frac{1}{2}p^2(y)V'^2(y) - \frac{1}{2}\bigl[V'(y)p^2(y)\bigr]'\right\}\exp\bigl[-V(y)\bigr]\,dy\right\} \Big/ \left\{\int_{-\infty}^{+\infty}p^2(y)\exp\bigl[-V(y)\bigr]\,dy\right\}. \tag{A.7}$$

Since

$$\begin{aligned}\int_{-\infty}^{+\infty}&\bigl[V'(y)p^2(y)\bigr]'\exp\bigl[-V(y)\bigr]\,dy \\ &= V'(y)p^2(y)\exp\bigl[-V(y)\bigr]\Big|_{-\infty}^{+\infty} \\ &\quad + \int_{-\infty}^{+\infty}p^2(y)V'^2(y)\exp\bigl[-V(y)\bigr]\,dy \\ &= \int_{-\infty}^{+\infty}p^2(y)V'^2(y)\exp\bigl[-V(y)\bigr]\,dy,\end{aligned}$$

Eq. (A.7) can be rewritten as

$$\lambda = \frac{\int_{-\infty}^{+\infty}p'^2(y)\exp[-V(y)]\,dy}{\int_{-\infty}^{+\infty}p^2(y)\exp[-V(y)]\,dy}. \tag{A.8}$$

Assume $p(y) = d_0 + d_1 y + \cdots + d_n y^n$ and the order n is an integer, we obtain

$$\bigl([K] - \lambda[M]\bigr)\{d\} = 0, \tag{A.9}$$

with eigenvectors $\{d^i\} = [d_0^i, d_1^i, \ldots, d_n^i]$ corresponding to eigenvalues $\{\lambda\} = [\lambda_0, \lambda_1, \ldots, \lambda_n]$ for $i = 0, 1, \ldots, n$. The integer n is not increased in the iterative process until the preceding values of λ_i approximate the next ones within the tolerance error. The elements of matrices $[M]$ and $[K]$ are

$$m_{ij} = \int_{-\infty}^{+\infty}y^{i+j}\exp\bigl[-V(y)\bigr]\,dy > 0,$$

$$k_{ij} = \int_{-\infty}^{+\infty}ijy^{i+j-2}\exp\bigl[-V(y)\bigr]\,dy \geqslant 0,$$

where $i,\ j = 0, 1, \ldots, n$. The matrix $[M]$ is positive definite and the matrix $[K]$ is semi-positive definite. The minimal eigenvalue λ_0 is zero. The minimal positive eigenvalue λ_1 describes the main speed of the system tending to the steady state solution of Eq. (A.3), what we call the receiver response speed.

From Eq. (A.9), we can obtain the eigenfunctions $u_i(y) = p_i(y)\exp[-V(y)/2]$ corresponding to the eigenvalue λ_i for $i = 0, 1, \ldots, n$, where $p_i(y) = d_0^i + d_1^i y + \cdots + d_n^i y^n$. The eigenvectors $\{d^i\} = [d_0^i, d_1^i, \ldots, d_n^i]$ are normalized. Because L is a Hermitian operator, eigenfunctions $u_i(y)$ and $u_j(y)$ are

orthogonal

$$\int_{-\infty}^{+\infty} u_i(y)u_j(y)\,dy = \delta_{ij}, \tag{A.10}$$

where $i, j = 0, 1, \ldots, n$. Hence, $\rho(y,\tau)$ can be expanded, according to eigenfunctions $u_i(y)$ and eigenvalues λ_i, as

$$\rho(y,\tau) = \sum_{i=0}^{n} C_i u_i(y) \exp\bigl[-V(y)/2\bigr] \exp[-\lambda_i \tau],$$

where C_i are normalization constants deduced from the orthogonal condition of eigenfunctions [39]. Note the scale transformation in Eq. (A.1), $\rho(x,t)$ can be represented as

$$\rho(x,t) = \sum_{i=0}^{n} C_i u_i(x) \exp\bigl[-\tau_a V(x)/(2D)\bigr] \times \exp[-\lambda_i t], \tag{A.11}$$

with the real eigenvalues $\lambda_i = \lambda_i'/\tau_a$ in the timescale of t and λ_i' derived from Eq. (A.9).

References

[1] R. Benzi, A. Sutera, A. Vulpiani, J. Phys. A: Math. Gen. 14 (1981) L453.
[2] K. Wiesenfeld, F. Moss, Nature (London) 373 (1995) 33.
[3] A.R. Bulsara, L. Gammaitoni, Phys. Today 3 (1996) 39.
[4] L. Gammaitoni, P. Hänggi, P. Jung, F. Marchesoni, Rev. Mod. Phys. 70 (1998) 223.
[5] F. Moss, L.M. Ward, W.G. Sannita, Clin. Neurophysiol. 115 (2004) 267.
[6] G.P. Harmer, B.R. Davis, D. Abbott, IEEE Trans. Instrum. Meas. 51 (2002) 299.
[7] G.P. Harmer, D. Abbott, Microelectron. J. 32 (2001) 959.
[8] J.J. Collins, C.C. Chow, T.T. Imhoff, Phys. Rev. E 52 (1995) R3321.
[9] J.J. Collins, C.C. Chow, A.C. Capela, T.T. Imhoff, Phys. Rev. E 54 (1996) 5575.
[10] F. Chapeau-Blondeau, Phys. Rev. E 55 (1997) 2016.
[11] K. Wiesenfeld, F. Jaramillo, Chaos 8 (1998) 539.
[12] S. Barbay, G. Giacomelli, F. Marin, Phys. Rev. Lett. 85 (2000) 4652.
[13] I. Goychuk, P. Hänggi, Phys. Rev. E 61 (2000) 4272.
[14] L.B. Kish, G.P. Harmer, D. Abbott, Fluctuation Noise Lett. 1 (2001) L13.
[15] G.P. Harmer, D. Abbott, Microelectron. J. 31 (2000) 553.
[16] M.D. McDonnell, N.G. Stocks, C.E.M. Pearce, D. Abbott, Electron. Lett. 39 (2003) 1287.
[17] V.S. Anishchenko, M.A. Safonova, L.O. Chua, Int. J. Bifur. Chaos 4 (1994) 411.
[18] A.N. Grigorenko, P.I. Nikitin, G.V. Roshchepkin, J. Exp. Theor. Phys. 85 (1997) 343.
[19] K. Park, Y. Lai, Z. Liu, A. Nachman, Phys. Lett. A 326 (2004) 391.
[20] S. Morfu, J.M. Bilbault, J.C. Comte, Int. J. Bifur. Chaos 13 (2003) 233.
[21] J.C. Comte, S. Morfu, Phys. Lett. A 309 (2003) 39.
[22] X. Godivier, F. Chapeau-Blondeau, Int. J. Bifur. Chaos 8 (1998) 581.
[23] F. Apostolico, L. Gammaitoni, F. Marchesoni, S. Santucci, Phys. Rev. E 55 (1997) 36.
[24] F. Duan, D. Rousseau, F. Chapeau-Blondeau, Phys. Rev. E 69 (2004) 011109.
[25] B. Xu, F. Duan, F. Chapeau-Blondeau, Phys. Rev. E 69 (2004) 061110.
[26] J. Mason, J.F. Lindner, W. Ditto, J. Neff, A. Bulsara, M. Spano, Phys. Lett. A 277 (2000) 13.
[27] A.S. Asdi, A.H. Tewfik, IEEE Int. Conf. Acoustic Speech Sig. Proc. 2 (1995) 1332.
[28] M.F. Carusela, R.P.J. Perazzo, L. Romanelli, Phys. Rev. E 64 (2001) 031101.
[29] F. Duan, D. Abbott, Q. Gao, Fluctuation Noise Lett. 5 (2005) L127.
[30] M. Morillo, J. Gómez-Ordóñez, Phys. Rev. E 51 (1995) 999.
[31] J. Casado-Pascual, J. Gómez-Ordóñez, M. Morillo, Phys. Rev. Lett. 91 (2003) 210601.
[32] W. Zheng, Phys. Rev. A 44 (1991) 6443.
[33] F. Zeng, Q. Fu, R. Morse, Brain Res. 869 (2000) 251.
[34] A.R. Bulsara, A. Zador, Phys. Rev. E. 54 (1996) R2185.
[35] N.G. Stocks, R. Mannella, Phys. Rev. E 64 (2001) 030902.
[36] P.A. Tass, Chaos 13 (2003) 364.
[37] J.G. Proakis, Digital Communications, third ed., McGraw–Hill, New York, 1995.
[38] T.C. Gard, Introduction to Stochastic Differential Equations, Marcel Dekker, New York, 1998.
[39] H. Risken, The Fokker–Planck Equation: Methods of Solution and Applications, Springer Series in Synergetics, vol. 18, second ed., Springer-Verlag, Berlin, 1989.